HEAT TRANSFER MODELLING OF A SUPERCAPACITOR STACK

Ran Zhao

Bachelor of Engineering
Mechanical Engineering

Department of Electronic Engineering
Macquarie University

Novermber 07, 2016

Supervisor: Dr. Ann Lee

ACKNOWLEDGMENTS

I gratefully acknowledge the help of my supervisor Dr. Ann Lee. I would like to express my gratitude to all those who have helped me during the writing of this thesis. I do appreciate his patience, encouragement, and professional instructions during my thesis project process at Macquarie University.

STATEMENT OF CANDIDATE

I, Ran Zhao, declare that this report, submitted as part of the requirement for the award of Bachelor of Engineering in the Department of Electronic Engineering, Macquarie University, is entirely my own work unless otherwise referenced or acknowledged. This document has not been submitted for qualification or assessment an any academic institution.

Student's Name: Ran Zhao

Student's Signature: 

Date: 07/11/2016

ABSTRACT

Supercapacitors, also known as ultracapacitors, electrochemical capacitors or electrical double-layer capacitors (EDC), are novel energy storage devices which operate between capacitors and batteries with respect to power performance and energy storage. Supercapacitor stacks have a wide range of industrial applications such as temporary power storage devices in electric vehicles or energy sources to reduce strains on batteries. Since a single supercapacitor cell can only produce a relatively low maximal operating voltage, it is common to connect a large number of individual supercapacitors in series to achieve the power requirement which has been call supercapacitor stack. Since the supercapacitor stack may operate under critical condition on industrial and commercial environment, the cooling strategy and cell arrangement has a significant impact of the operation temperature of individual capacitors within the stack. This thesis project simulates the thermal model supercapacitor stacks with different air flow rates and cell arrangements by apply lumped element model method. It is hoped this project will provide a better cell arrangemnt which has better cooling effect for supercapacitor stack.

Contents

List of Figures

List of Tables

Chapter 1

Introduction

1.1 supercapacitor Stack

Traditional lead-acid batteries use increasingly obsolete technology and toxic chemical energy storage. Although the traditional chemical batteriescan meet the needs of certain applications. But it has insurmountable limitations on safty, reliablity, low instantaneous release of high power and long service duration of the emerging applications. Industries are searching for alternatives in the process,supercapacitor is one of the most efficient, economical and environmentally friendly alternative energy storage solutions available. Supercapacitors have characteristics of high power density, extremely large capacitance, long cycle life and high charge and discharge efficiency. By combining multiple supercapacitor cells into a single module, supercapacitors stacks can reach or exceed the energy and power requirements of multiple demanding applications. The supercapacitor module provides reliable, low-cost solutions for UPS, telecommunications, automotive, transportation, and other applications, with robust performance in hundreds of thousands of cycles [1].

1.2 Scope

After the cooling issue has been addressed and how important it is, the better array of supercapacitor stack can be developed to reduce long term cost and increase reliability. It has been shown that the temperature has a great influence on the aging mechanism of supercapacitors and, by consequence, on the lifetime of the system. The short-term goal in the project is using CFD to modelling the thermal condition of a supercapacitor stack under different variables in the computer. The thermal characteristics of the stacks will be determined after finish this project. For the long-term target, the better solution of cooling system in supercapacitor stack maybe found for different purposes [2] [1].

Chapter 2

Background and Related Work

2.1 What is supercapacitor?

Supercapacitors also known as ultercapacitors, electrochemical capacitors or electric double-layer capacitors (EDLCs). The basic structure for conventional capacitors are made by two electrically conducting plates or electrodes separated by a dielectric, such as air, silicon or ceramic. The positive and negative charges stay in opposite side of the plates to develop an electric filed from the dielectric composition. However, compare the charge is stored location is different between a supercapacitor and a conventional capacitor. A double terminal supercapacitor is equivalent to two conventional capacitors in series because charges are stored at the surface between an electrolyte and an electrode (each side can be considering as a single capacitor). The characteristics for supercapacitor can fill the gap between conventional battery by featuring lower power density but higher energy density and capacitors which has lower energy density and higher power density. It named by supercapacitor because large amount electrodes in the surface and short distance between the two kind of charges inside of the supercapacitor. There are several advance futures, such as free maintenance, high power density and long lifecycle [3] [4].

2.2 Type of supercapacitors

Supercapacitors can be defined to two types based on operating structure:

- Electric double-layer capacitors (EDLCs): Large surface area of the electrode material, the use of electrodes and electrolyte solution Coulomb electrostatic charge caused by the phenomenon of separation. Thus the formation of electric double layer to achieve the purpose of storage of electricity. As the potential changes, that is caused by changes in surface energy of the electrode. Therefore, the arrangement of the two-layer is also relatively change, and form the same charge-sharing phenomenon of the same capacitor [5] [6].
- Pseudo capacitors: The fast reversible Faraday charge transfer is used to storage

electrode and electrolyte. The electrochemically actives action on the surface of the electrode are used to make reversible reaction for redox or elecyroadsorption or desorption. Because the charge transfer has involved. The charge storage is much larger than the conventional capacitors and electric double layer capacitors [6] [7].

2.3 Competitors

Lithium Ion Battery

High voltage is applied to the two plates, the positive and negative charges of the positive and negative plates of the supercapacitor will be respectively generated and the electric charge in the electrolyte will be redistributed by the electric field generated by the charge of the two plates. A counter electric charge is formed on the contact interface with the electrode at a very short gap in the opposite position to balance the electric field in the electrolyte to form a special electric double layer charge distribution structure. The super capacitor is obtained from the porous carbon based electrode material Charge area, and its surface area per gram can be as high as 2000 square meters. While the distance separating the charge in the supercapacitor is determined by the size of the ions in the electrolyte and is less than 10 angstroms. The large surface area plus a very small distance between the charges makes the supercapacitor very capacitive. With the super capacitor discharge, the positive and negative plates of the charge is discharged from the external circuit, the electrolyte at the interface of the charge is correspondingly reduced, so the charge and discharge process is always the physical process, there is no chemical reaction. So the performance is stable, and the use of chemical reactions of the battery is different [8] [9].

People have tried to develop lithium-ion rechargeable lithium-ion rechargeable battery, and in a large number of literature has introduced their classification and characteristics.Some of the commercialization of lithium secondary batteries in the 20th century, including$LiTiS_2, LioS_2$ and $LiLixMnO_2$.
The mid-90s, Israel Tadiran company developed the latest commercial system of AA batteries, and used in mobile phones. Because of security issues, $LiTiS_2$ and $LiMoS_2$ system is not enabled.TheLi_xMnO_2 system is considered safe due to inherent safety mechanisms [6], but to obtain long cycle life rechargeable batteries require a long charging time. At present, graphite is introduced instead of lithium metal as anode material and by lithiated transition metal oxide $LiMO_2$ as a cathode material, the rapid development of battery technology, making the reversible, high-energy-density lithium-ion battery market.At present, based on graphite.$LiC0O_2$ Li-ion battery system has the most widely use, such as portable electronic devices, mobile phones, laptops and digital cameras.The main cell reaction occurs in a reversible Li insertion / extraction cycle between the two layered compounds. In order to ensure the anode stability between the positive electrode material and the electrolyte solution [10] [11].

The overcharge voltage of $LiC0O_2$ is limited to 4.2 V, which means that only half of the theoretical capacity (140 mAWg) of the cathode material can be extracted during the reaction. It due to the first order phase structure between $LiC0O_2$ and $Li_{0.5}C0O_2$ .As

mentioned above, in lithium-ion batteries, Li is derived from a cathode material, which ensures a theoretical study of lithium ion batteries and supercapacitor electrode materials with respect to the lithium metal-based battery, which has long-lasting storage life and perfect safety performance.The first reaction process in the cell is always the charging process, that is, oxidation reaction and LiC002 de-lithium, relative to the discharge of a reduction reaction and lithiation of graphite. Reversible Li metal insert graphite, the formation of LiC_6 as the final product, the reaction equation is [10] [11] :

$$LiCoo_2 \rightleftharpoons \frac{1}{2}Li^+ + Li_{0.5}CoO_2 \tag{2.1}$$

The intercalation of Li into graphite occurs in the first-order phase transition of different phases, such as LiC_{24}, LiC_{27} and $LiCl_2$. The first polarization of the graphite electrode occurs in any polar aprotonic Li salt solution which consumes irreversible charges, reducing the species in the solution.These processes may lead to the formation of a passivation film, which prevents the irreversible reaction from taking place and provides conditions for the formation of ".C6 metastable structures" [12] Thus, in order to provide charge for the Li-ion and the passivated graphite surface film, each lithium ion battery must contain a lithium source-cathode material ($LiMO_2$). In developing practical lithium-ion batteries, a key task is to reduce the amount of reversible charge consumption, that is, to reduce the amount of additional cathode material [12].

Lithium Ion Battery

Fuel Cell (FC) is a power plant that converts chemical energy from fuel directly into electrical energy by electrochemical reaction. There are many types fuel cells, include Proton Exchange Membrane Fuel Cell (PEMFC), Phosphoric Acid Fuel Cell (PAFC), Alkaline Fuel Cell (AFC), solid oxide Fuel cell (SOFC) and molten carbonate fuel cell (Molten Carbonate Fuel Cell, MCFC). The major components for the proton exchange membrane fuel include: Membrane Electrode Assembly (MEA), bipolar plate and sealing components. Membrane electrode assembly is the central component of electrochemical reaction, which consists of cathode and anode porous gas diffusion electrode and electrolyte membrane. Electrolyte membrane on both sides of the oxidation reaction occurred with the oxygen reduction reaction. In a hydrogen cell, hydrogen and oxygen are the fuel and oxidant, respectively. Hydrogen is oxidized at the anode, and protons enter the electrolyte,

$$H_2 \rightarrow 2H_+ + 2e^- \tag{2.2}$$

At the cathode, the oxygen gas reacts according to,

$$O_2 + 4e^- \rightarrow 20^{2-} \tag{2.3}$$

Electrons flow from the anode to the cathode in the external circuit and can be used to power a device. The net reaction of the fuel cell is given by,

$$H_2 + \frac{1}{2}O_2 \rightarrow H_2O \tag{2.4}$$

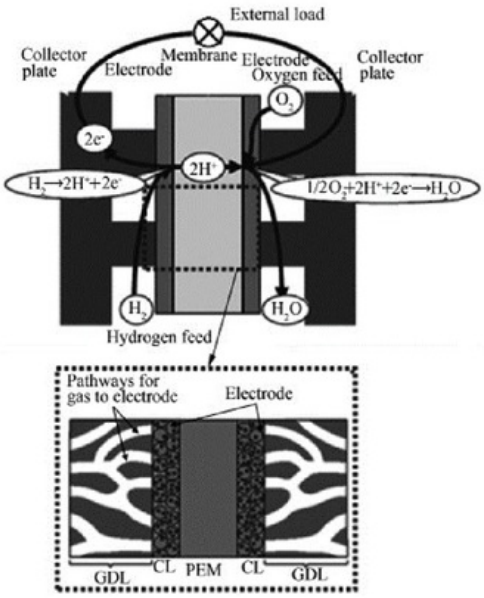

Figure 2.1: Principle of a PEMFC.

In order to reach the power requirements of a given application, fuel cells typically consist of hundreds of cells connected in series to form a fuel cell stack. Therefore, compare with other chemical energy storage device, fuel cell uniformity is very important. Fuel cells have a similar principle to those of primary batteries, but require a relatively complex system which including fuel supply, oxidant supply, hydrothermal management and electrical control. In theory, as long as the external constant supply of fuel and oxidant, the fuel cell can continue to generate electricity. Fuel cells are widely used in civil and military fields, such as transportation, portable power supply, distributed power station, aviation / day and underwater vehicles. At present, fuel cell vehicles, power plants and portable power are all in the demonstration stage. In the special field which focus on life and reliability, the existing fuel cell technology can meet the application requirements [11] [13].

Other Energy Storage Device

Beside the foregoing electro-chemical energy storage devices. There are many other energy storage devices have been applied in different industrial applications, such as closed batteries (odium sulphur, lead acid and sodium nickel chloride), zinc-bromine batteries and vanadium redox batteries. The very special working principle of redox flow batteries drop attentions from academic researchers and industrial applications. There are five advantages for redox flow battery: [3]

1. Rated power and rated power for redox flow battery are independent which means it can increase the amount of electrolyte, in order to achieve the purpose of increase the battery capacity.

2. No require phase change during the charging and discharging stage. Redox flow battery takes liquid phase reaction during this period.

3. Infinite life cycle. Because the electrolyte is recycled, after long time use the cell membrane resistance is the only changed perimeter. Redox flow battery can be fully discharge without any damage.

4. Redox flow battery has simple structure, cheap material price, low cost of replacement and maintenance.

5. Short energy transfer time. By changing the electrolyte, redox flow battery can recharge instantly.

The table on appendix summarizes and compares the characteristics of different common electrochemical energy storage systems as provided [14].

2.4 supercapacitor market outlook

With the rise of green energy industry, clean and pollution-free renewable energy and electric vehicles is bound to become the future development goals. Energy storage devices will be the development of renewable energy and electric vehicles is the most critical technology, super capacitor with high power density, fast charge and discharge capacity, long life cycle and other advantages. Therefore, it can be used as a high-power power output, an unstable power balance and an extended life in an energy storage device, and a complementary effect with a lithium-ion secondary battery. However, to enhance the energy density of super capacitors has been the focus of research and development. The high specific surface area of the graphene itself and the rich mesoporous structure contribute to the rapid migration of electrolyte ions to the graphene surface, and make full use of the specific surface area to store charge and improve the energy density of the supercapacitor. The literature shows that the current performance of graphene supercapacitor can already achieve the energy density of thin lithium ion secondary battery and aluminum electrolytic capacitor power density, and low-cost production potential. I believe graphene super capacitor in the application of energy storage will be just around the corner. The table showns commerical supercapacitor performance [15] [16] [17] [3].

Table 2.1: Commerical supercapacitor cell performance

[18]

Company	Electrolyte	Performance	R ($m\Omega$)	($Wh \setminus kg$)	($W \setminus kg$)
Maxwell	Organic electrolyte	2.7V,3 000F	0.29	6	5 900
Maxwell	Organic electrolyte	48V,165F	6.3	3.9	3 300
Esma	Water-based electrolyte	1.7V,50 000F	0.4	8	80
NCC	Organic electrolyte	2.5V,2 300F	1.2	4.07	1 275
Ness	Organic electrolyte	2.7V,3 000F	0.26	5.73	3 040
Ness	Organic electrolyte	48V,165F	5.6	3.4	6 500
SPS	Organic electrolyte	2.7V,3 000F	0.26	5.7	6 348
SPS	Organic electrolyte	48V,165F	6	2.8	2 425
Aowei	Organic electrolyte	2.7V,3 500F	0.3	4.8	3 940
Aowei	Water-based electrolyte	1.5V,80 000F	0.45	5	193
Jurong-newpower	Water-based electrolyte	1.5V,80 000F	0.3	5.25	225

Chapter 3

Methodology

3.1 Computer Fluid Dynamics simulation

Computer fluid dynamics (CFD) combine computer science, fluid dynamic and mathematic. It analysis

The governing equations of fluid flow express the mathematical form of the physical conservation laws:

1. Fluid mass conservation.
2. The rate of change of the momentum of the fluid particles is equal to its combined force (Newton's second law).
3. The rate of change in the energy of the fluid particles is equal to the sum of the rates of particle heating and work (the first law of thermodynamics).

The fluid is a continuous medium. Analysis of fluid flow at a macro scale (eg, 1 m) can ignore the molecular structure and molecular motion of matter. The physical quantities describing the properties of the fluid, such as velocity, pressure, density, temperature, and their spatial and temporal derivatives, can be the average for sufficient number of molecules. Then a fluid particle or a point in the fluid refers to the smallest possible fluid unit whose macroscopic properties are not affected by a single molecule [19].

3.2 Numerical model

This thesis conducted using ANSYS Workbench to make the computational modelling. ANSYS CFX software package is used to process the heat transfer simulation [3]. Another software ANSYS Workbench meshing tool can produce vertically meshing of the object. Since the ANSYS Workbench has FLUENT and CFX which both have capability to simulate the thermal condition of the supercapacitor stack. After evaluate the complexity, solving time and other perimeter for the thermal simulation in the researching stage of this program [20]. CFX has chosen to be the primarily simulation software to simulate

the thermal condition for the supercapacitor stack because it user-friendly interface, easy to examine the object and post simulation data analysis. Before begin this project, two demotion models are created to reduce the solving time and easy to be created. However, CFX can only be used to three demotion object which can be created by Creo. For the purpose to solve the two-demotion model, only one mesh element exists along the thickness of the heat transfer domain, so the mesh of the object must create very careful and precisely [13].

3.2.1 Lumped model

The lumped thermal models can be used to solve the average temperature rather than find the spatial temperature distribution of supercapacitors. [20]Temperature changes within the object has to small compared to the temperature gap between the object and the environment which this model can be applied. For example, a large diameter cycling currents which the temperature gradient of the object is remarkably small than the outside surface temperature. [21]The benefits of using lumped thermal model to analysis the heat transfer of supercapacitor because minimum computation cost, inherent simplicity and easy data analysis. In some concentrated model, called single temperature model which only assess the average temperature of device and comparing with the experimental temperature [20]. However, this approach may involve significant error, because the experiment temperature is usually available from the outside wall of the thermocouple connected to the device and can be different from the average temperature [22]. In order to obtain better estimates that can evaluate two temperature values, the core and outside wall temperature, which is called double temperature model. Core temperature is usually higher than the outside wall temperature a few degrees.

Single temperature modelsl

The temperature of the supercapacitor increase due to the heat generation during the charging and discharging stage. The heat generated is gradually dissipated to the surrounding. The heat generated in the supercapacitor due to Joule heating equal to the heat dissipated to the surrounding after the object able to steady state which took few initial charging and discharging cycles [20]. Joule heating can be calculated in two methods [20]: One is make an equivalent circuit model to calculated Joule heating in the resistances for the supercapacitor. Another is calculated by assuming it to be equal to the energy loss measured in one charge/ discharge cycle.In the former method, the heat balance is shown under equation

$$P_{TH} = \frac{\Delta T}{R_{th}} = \dot{q}_{gen} = \dot{q}_{Joule} = I^2 R_s \Delta T = I^2 R_S R_{th} \tag{3.1}$$

ΔT: the difference between the capacitor temperature and the ambient temperature
I: the current assumed to be constant
R_s: the equivalent dc resistance
R_{th}: the equivalent thermal resistance

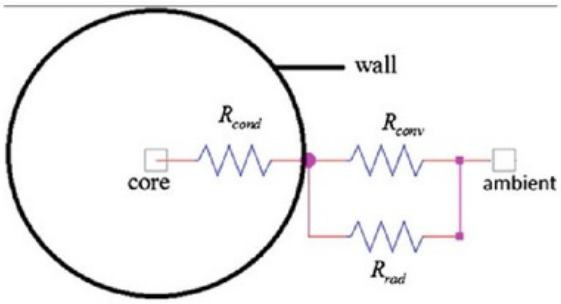

Figure 3.1: Equivalent circuit for heat transfer in a commercial supercapacitor.

The left side of the equation is the heat loss rate to the environment, and the right side of the equation is the heat generation rate due to Joule heating [22].
The average temperature as a function of time can be calculated,

$$\Delta T = I^2 R_S R_{th}(1 - exp(-\frac{t}{\tau})) \tag{3.2}$$

τ: the thermal time constant (the time required to reach steady state temperature). R_{th}: the thermal resistance
The exponential decay term represents the gradual rise of temperature to steady state. However, such models only account for the Joule heating and not reversible heat generation.

$$R_{th} = R_{cond} + \frac{1}{\frac{1}{R_{conv}} + \frac{1}{R_{rad}}} \tag{3.3}$$

The thermal resistance is a combination of the conduction, convection and radiation thermal resistances,
R_{cond}: the conduction resistance
R_{conv}: the convection resistance
R_{rad}: the radiation resistance
An example thermal resistance circuit is shown

Conduction heat transfer occurs from the core to the supercapacitor wall while both convection and radiation heat transfer are from the wall to the ambient. The thermal resistances are evaluated from:

$$R_cond = \frac{l_{cond}}{kS_{cond}} R_{conv} = \frac{1}{h_{conv} S_{conv}} R_{rad} = \frac{1}{h_{rad} S_{rad}} \tag{3.4}$$

l_{cond}: the conduction length,
k: the average thermal conductivity of the supercapacitor component materials.
S_{cond} : the average areas for conduction heat transfer
S_{cony} : the average areas for convection heat transfer
S_{rad} : the average areas for radiation heat transfer

h_{conv}: the average convection heat transfers coefficients
h_{rad}: the average radiation heat transfers coefficients
The parametersl_{cond}, S_{cond}, S_{rad} and k can be determined from the geometry of a device and the thermal conductivity of the material [23] [24]. The convection heat transfer coefficient, often obtained from correlations, depends on whether the convection is forced or natural. Nusselt number (Nu) correlations are often used to evaluate the heat transfer coefficient [3],

$$Nu = \frac{h_{conv}D}{k} Nu = \alpha Re^{\beta 1} Pr^{\beta 2} \tag{3.5}$$

D: the outer diameter of the casing
k: the thermal conductivity of air.
Re: the Reynolds number
Pr: the Prandtl number
An approximate relation between h_{conv}: and air velocity is often used,

$$h_{conv} = 11\sqrt{\frac{v+0.25}{0.25}}\dot{q}_{rad} = \varepsilon\sigma S_{rad}(T_s^4 - T_a^4) = h_{rad}S_{rad}(T_s - T_a) \tag{3.6}$$

The radiation heat transfer coefficient h_{rad} is evaluated from,
ε: the emissivity
S_{rad}: the surface area
T_s: the temperature of the outer surface of the wall
σ: the Stefan-Boltzmann constant
T_a: the ambient temperature
h_{rad}: the heat loss due to radiation
For practical applications, the total heat transfers coefficient h_{tot} (combining h_{cony} and h_{rad}) can be

$$h_{tot} = 5 + 17(v + 0.1)^{0.66} \tag{3.7}$$

Models for transient temperature accounting for reversible heating as well as heat loss to the ambient in addition to irreversible heat losses have been employed,

$$\frac{dT(t)}{dt} = \frac{1}{C_{Heat}}[\frac{dq_{Joule}(t))}{dt} + \frac{dq_{rev}(t))}{dt} - S_{conv}h_{conv}(T(t) - t_a)] \tag{3.8}$$

The reversible heat generation term. This equation was simplified by replacing all the parameters with three non-dimensionalized parameters by dEntremont et al. The future CFD experiment will be based on this equation to determine the heat transfer for the supercapacitor stack [1].

Double temperature modelsl

Another model can be used to is double temperature model.

3.3 Electro-thermal model

Another model can be used to is double temperature model. The steady-state temperature values in the wall and centre of the supercapacitors instead of an overall average temperature has been studied. The heat generation $\dot{q}_{gen}$ is obtained in the way described for single temperature models. Under this condition, $\dot{q}_{gen}$ equals the heat loss rate P_{th}.

$$P_{th} = \dot{q}_{gen} = h_{eq} S_{conv} (T_s - T_a) \tag{3.9}$$

Assuming only convection at the outer surface, the surface temperature of the casing T_s is derived using,
h_{eq}: the equivalent heat transfer coefficient
T_a: the ambient temperature

3.4 Numerical simulation of the process

The major task of computational fluid dynamics is the numerical simulation of fluid mechanics. Numerical simulations is a value experiment which implemented on a computer to perform a particular physical computation through numeric computation and image display to perform a virtual number of experiments. Numerical simulation involves the following steps [25].

1. Establish reflect the problem (engineering problems, physical problems, etc.) the nature of the mathematical model. It is the starting point of numerical simulation to establish the differential equation and the corresponding condition for solving the problem [26]. The mathematical model of Newtonian fluid flow is the well-known N-S equation and its corresponding solution condition

2. Mathematical model to be solved after the establishment of the problem is to seek high efficiency, high accuracy of the calculation method [26]. The calculation method includes not only the discretization and solving method of mathematical equation, but also the establishment of computational grid and the processing of boundary condition.

3. After determining the calculation method and the coordinate system, the preparation process and the calculation is the main body of the whole work. When the solution of the problem is more complex, such as solving nonlinear N-S equation, also need to be verified through experiments.

4. Finally, the image display of the flow field is an indispensable part when the calculation is done. With the increasingly deep and complicated problem, the calculation results are more complicated and difficult to grasp. Only the results of numerical calculation in a variety of images and curves in the form of output can effectively determine the correctness of the results, and then come to conclusions and access to

the required data. With the development of the computer image display system and the corresponding software, the image of the flow field has been developed rapidly in the aspects of fast and timely, three-dimensional scanning and vivid image [26].

After understanding the principle and process of numerical simulation, it can better understand the operation of CFD software and achieve the task successfully. Commercial CFD software usually computational fluid mechanics more mature numerical method, a typical configuration and operation process [17]. All commercial CFD software includes three main parts: pre-processing, calculating and post-processing. The pre-processing is to input the flow problem into the CFD program through the operation interface, and then convert the input data into the appropriate format suitable for the operation part. There are few steps for the pre-processing need to be follow to solving CFD problems [17].

1. Computing domain which is the definition of the relevant geometric area,
2. Mesh generation which divides the computational domain into smaller, non-overlapping subdomains or cells (grids),
3. Select the physical and chemical phenomena of the model,
4. Define the appropriate boundary conditions at the elements that overlap and contact the boundary.

The solution of the flow problems (velocity, pressure, temperature, etc.) are defined at the node of each element. The accuracy of the CFD is determined by the number of grid cells. The accuracy of the solution, the necessary computer hardware and the computational time depend on the degree of detail of the mesh [27]. The best mesh is non-uniform: the interval between the point-to-point change is quicker, the mesh is finer, and the range of change is relatively slow. One of achievement of CFD development is adaptive mesh generation. Eventually such programs will automatically subdivide the mesh in rapidly changing regions. Currently in advanced software, this target has not been achieved which needs CFD users have the skills to design the grid to meet the problem-solving accuracy and reduce cost requirements [3]. Grid generation is an important branch of computational fluid dynamics (CFD), and it is one of the key technologies faced by CFD as an effective tool for engineering application. Successful meshing of complex shapes depends on the collaboration and effort of the professional team. Experience shows that more than 50 per cent of time spent on CFD projects are used to define computational domain geometry and mesh generation. Numerical method has three different types: finite difference method, finite element method and spectral method [4]. All those methods are under those three basic steps: the simple function of the approximate form of unknown variables, approximation into the flow control equation and discretization and mathematical processing algebraic equations; The major difference between those three different methods is that the approximation of the flow variables and the discrete processing are different. The finite difference method uses the point samples on the grid nodes to describe the variables of unknown flow problems. The finite difference method uses the Taylor series

expansion truncation to obtain the approximate expression of the derivative of the flow variable at one point, which uses this and the samples of the neighbouring points. The algebraic equation of the node flow variable is obtained by replacing the derivatives with the finite difference in the control equation [3].

The finite element method uses a simple piece function (eg, linear or quadratic) to describe local variations of unknown flow variables within a cell. The exact solution satisfies the control equation exactly, but it cannot be established exactly after the piecewise approximation function is substituted into the equation, so this error is measured by defining the residuals. A set of weight functions is then used to multiply and integrate with the residual (or error) terms to eliminate the residuals in the sense of weighted integrals and to make the integral zero. The result is a set of approximate algebraic equations with unknown coefficients. Finite element theory was originally developed for the analysis of structural stresses, and the application of standard fluid finite element methods has been described.Spectral method uses Fourier series or Chebyshev polynomial series truncation to approximate the unknown quantity [28]. Spectral method is different from finite difference method and finite element method, it is not a local approximation; approximation is valid for the whole computational domain. By substituting the truncation series into the governing equations, the constraints of the equations produce algebraic equations about the coefficients of the Fourier series or Chebyshev series [28]. Similarly, the finite element method, the spectral method provides the constraint condition by using the concept of weighted residuals and the approximate function on the node which is consistent with the exact solution. Large-eddy simulation method to calculate the turbulence will use the concept of spectrum. The actual physical phenomena are complex and non-linear, so the iterative method is used to solve algebraic equations. The commonly used solutions is the algebraic equation T DMA line-by-line operator which can guarantee the pressure and the speed of the correct contact SIMPLE algorithm. Commercial CFD software also gives the user other options, such as the ST ONE algorithm and conjugate gradient method. As with pre-processing, there has been a lot of development work in the postprocessing area. Thanks to the increasing number of computers with superb graphics capabilities, excellent CFD packages are equipped with data visualization tools. This includes: Geometry and Grid Display, Vector, Contour or Shadow, 2D, 3D, Particle Traces, Image Processing (Moving, Rotating) , Zoom, etc.), colour image storage, printing, output [29]. Those configurations also include animations which dynamically display the results. In addition to graphics, all software has a data output function for further processing of data outside the software. Making the right decisions requires good modelling skills. In addition to the simplest of all problems, we need to make assumptions to reduce the complexity to the extent that can be carried out, while maintaining the characteristics of the problem. The appropriateness of the simplification introduced in those steps are determined in part by the quality of the information produced by the CFD.

Chapter 4

Verification

4.1 Gird description

As an important part of the finite element model, the mesh segmentation requires a lot of work and requires a lot of work. Different meshing methods have great influence on the calculation scale, calculation results and calculation accuracy. Therefore, it is necessary to study the finite element meshing. The ultimate goal of finite element analysis is to restore the mathematical behaviour of an actual engineering system. The analysis must be an accurate mathematical model of a physical prototype. In a broad sense, the model includes all nodes, elements, material properties, geometric properties, initial

Conditions, boundary conditions, etc., and other features used to express the physical system. In the narrow sense, the model generation only refers to nodes and cells that represent the spatial body domain and the actual system connection generation process, that is, mesh segmentation. In the process of establishing the finite element model, both the general and the narrow sense are involved in the problem of meshing. Some people have made statistics, in the three stages of numerical analysis, pre-treatment of about 40 per cent to 60 per cent of the total time, the numerical solution of about 5 per cent to 20 per cent, post-processing results accounted for about 30 per cent. If a purely artificial approach to the object of the discretization of the work will inevitably need to spend a lot of time, and when the model is complex, but also prone to error. Pre-process work is more complicated, but it is very important, which is the basis for the correct analysis of finite element. Therefore, to carry out a better analysis of object discretization of the work of discrete, in terms of numerical analysis workers, is of great significance [30].

Meshing requirementsl

Finite element mesh generation is the process of discretising objects in the working environment into units. Commonly used elements include one-dimensional rod elements and concentrated mass elements, two-dimensional triangular and quadrilateral elements, three-dimensional tetrahedrons, pentahedrons, pyramids, hexahedrons unit. The boundary shape of the main linear, straight type, curved type and surface type. Finite element

analysis requires several nodes on each edge or surface to satisfy the shape of the element, but also improve the accuracy, accuracy and speed of convergence. Different dimensions of the same object can be divided into a mixture of multiple elements of the grid. Meshing should follow the following guidelines [12].

1. Legitimacy. A node of a unit cannot fall into other units, the nodes on the unit boundary should be regarded as the node of the unit, and cannot be discarded.

2. Compatibility. The unit must fall within the area to be divided, cannot fall outside, and the unit union equals the area to be divided.

3. Coordination. The forces and moments on the element can be passed to the adjacent elements through the nodes. To ensure the unit coordination, it is necessary to satisfy that the node of a unit must be a node of an adjacent unit at the same time, not an interior point or a boundary point. The common nodes of adjacent units have the same degree of freedom properties, that is, the degrees of freedom must match.

4. Approximation accuracy. The vertices (including special points) of the area to be partitioned must be the nodes of the cell. The boundaries of the area to be partitioned (including special edges and planes) are approximated by the cell boundary.

5. Good shape of the unit. The best shape of the element is a regular polygon or a regular polyhedron.

6. Good transitional transition .The transition between the units should be relatively stable, otherwise it will affect the accuracy of the calculation results cannot even make the finite element analysis.

7. Adaptive mesh division .In the geometric cusp, stress, temperature and other changes in the local grid should be dense, other parts should be sparser, so you can ensure accurate and reliable calculation results.

8. Consistency. For the two connected quadratic elements, the cell corner can only relate to the cell corners and not with the intermediate nodes of the neighbouring cells.

4.2 Grid refinement

Mesh Quality Requirements

If the elements are ideal shapes (triangular element equilateral, quadrilateral square, hexahedral cube, etc.), errors and errors are less likely to occur in the calculation of the element stiffness matrix, but ideally throughout the model. It is difficult to divide the whole rule by regular elements. Therefore, different shapes of grids must be set up in the different positions of the model to improve the quality of the mesh [9]. Mesh quality is

very important for the accuracy of numerical analysis, especially for objects with complex shapes. For complex geometric entities and shells, it is first necessary to ensure that the mesh cells are strictly corresponding to the geometry; secondly, the cells are guaranteed to have high quality. There will be unit quality failure of the warning message, a serious error will lead to the calculation of interruption in the process of numerical calculation. Therefore, the establishment of grid quality standard system, for numerical analysis has very important significance. In general, the criteria for the quality of the content grid are different for different numerical analyses. For the general heat conduction analysis, the grid quality standard can be reduced appropriately, and for some nonlinear problems such as large deformation, contact, transient high-speed impact analysis and so on, a high-quality grid is needed. Since the quality of the initial mesh is not always satisfactory because the quality of the finite element mesh directly affects the accuracy and correctness of the numerical solution, the quality of the initial mesh is usually improved or optimized. Mesh quality improvement can be divided into two aspects: First, the adjustment of topological relations; Second, the node position adjustment. To check the quality of the mesh, you should first check whether there are duplicate nodes and cells. If two nodes or units need to be established at the same location, care should be taken. In most commercial engineering analysis software, there is a function to eliminate duplicate nodes within a certain tolerance range, and this function should be avoided if different nodes (such as contact problems) need to be generated at the same location. In order to ensure that the finite element analysis results are satisfactory to the user, the finite element mesh usually has the following conditions [31]:

1. All elements close to the ideal shape,
2. The main variables (temperature, velocity, etc.),
3. Uniform thickness between the grid transitions,

However, there are always some deformed cells in the mesh generated by the finite element mesh automatic generator. The more the problem domain is, the larger the proportion of the deformed mesh is. The goal of grid optimization is to change the quality of grid and improve the precision of calculation. At present, there are two main optimization methods :

1. Mesh finishing. The mesh is subdivided according to the density of the mesh and the requirements of the results,
2. Smooth treatment. The mesh topology is not changed, and the mesh quality is improved by perturbing the position of the nodes,

Laplacian smoothing technique is one of the earliest and most mature optimization methods . The core content of this paper is to keep the topological relation of the mesh, and the position of the whole inner node is perturbed to the centre of the polygon composed of its adjacent nodes, so that each unit is closer to the ideal shape. The perturbation

process is traversed all the internal nodes many times, can greatly improve the quality of the grid. The Laplacian smoothing mesh no longer has the basic properties of Delaunay triangulation [23]. In recent years, a variety of grid optimization methods have emerged, and adaptive mesh refinement is one of them. Firstly, the finite element analysis is performed on a sparse grid. Based on the results of the calculation, the grids of some areas need to be refined by some error indicator. After finishing the local adaptive mesh, the finite element analysis is carried out. Such a local mesh refinement can be repeated many times until the results meet the user requirements.

4.3 Boundary condition

Boundary condition refers to the variation of the first derivative or the first derivative of the solution on the boundary of the solution domain with the location and time. All CFD problems require boundary conditions, and transient conditions require initial conditions. The solution of the flow field is different, the boundary conditions and the initial conditions of treatment are not the same. In CFD simulation, the basic boundary conditions include: flow inlet and outlet boundary, given pressure boundary, wall boundary, symmetrical boundary and periodic boundary. Different solution models, boundary conditions are also different choices.

It is important to make appropriate boundary conditions under all section of the boundary of a computational domain Ω

$$n = n(s,t) \tag{4.1}$$

or the specification of surface stresses,

$$\sigma_n = \sigma \cdot n(s,t) = \sigma_a(s,t) \tag{4.2}$$

For the solution of the temperature field, the thermal balance on the boundary shows that either the temperature profile is specified,

$$T = T_a(s,t) \tag{4.3}$$

or a heat flux,

$$q = -n \cdot k\nabla T = q_a(s,t) \tag{4.4}$$

q_a represent both convective and radiative heat transfer along the object boundary The object‘s chemical species are based on the mass balance across the boundary.

$$C_i = C_{i,a}(s,t) \tag{4.5}$$

Mass flux

$$q_i = -n \cdot D_i \nabla C_i = q_{i,a}(s,t,C_{i,a}) \tag{4.6}$$

Initial conditions for all the primitive variables take the following generic forms:

$$u(x,0) = u^0(x)T(x,0) = T^0(x)C_i(x,0) = c_i^0(x) \tag{4.7}$$

where superscript 0 stands for a prescribed initial quantity [8] [17].

Symmetric boundary condition and periodic boundary condition are two kind of common boundary conditions.

Symmetric boundary condition

There is a physical symmetric for the examine object which can using symmetric boundary condition to half the solving duration. The vertical boundary velocity is zero and share the same physical perimeter as inside and outside of the boundary.

Periodic boundary condition

Periodic Boundary Conditions (PBC) is a kind of boundary condition, which reflects how to use the boundary conditions to replace the selected part (system) to be influenced by the surroundings (environment). Can be seen as if the removal of the surrounding environment, maintaining the system should be added to the conditions, can also be seen as part of the nature of the expression to promote the nature of the overall. Mainly used for mathematical modeling and computer simulation, will have a temporal and spatial periodicity of the physical problem is reduced to the unit for processing. Common Periodic Boundary Conditions

1. Continuity boundary the field values on the source and target boundaries are equal
2. Antiperiodicity boundary, the source and target field values on the opposite sign,
3. Floquet periodicity boundary, the difference between the field values at the source and target boundaries is a phase factor. The phase factor is determined by the distance between the wave vector and the boundary. The Continuity and Antiperiodicity boundaries can be thought of as two special cases of the Floquet periodicity boundary in the case where the phases are 0 and Π, respectively,
4. Cycle symmetry boundary, source and target boundaries on the difference between the field value of a phase factor, the phase factor corresponding to the calculation by the domain of the fan angle and angle mode number.

Since the 2 D model is applied to study the heat transfer in the supercapacitor stack to simulate the real 3D model, the model is simplified to an axisymmetric task by using suitable boundary condition. Maxxwell supercapacitor stacks are used as real world model which provide one of two model in the simulation. The model used in this project and summary of boundary conditions are shown. As shown on picture, model change the supercapacitor cells arrangement which is close to each other without any angle. Those two models share same total volume, in two dimension is the space, which represent same

number of supercapacitor cells are carried. The inlet for both model are $2m \setminus s$,$4m \setminus s$ and $6m \setminus s$ as boundary condition to exam thermal model for the stack under different air flow rate. A non- pressure opening is specified at the air outlet of the fluid domain. An opening boundary condition is used instead of outlet boundary condition in order to allow both-direction fluid flow, and is a better reflection of the real applicate condition. Those half circles represent the wall of each supercapacitor cells which produce $1.5833 \times 10^4 W \setminus m^2$ heat flux as boundary condition to all vertical surface. However, based on the super capacitor is smaller than the diameter of the longitudinal spacing. The fluid domain is divided into cycle without cutting the super capacitor is impossible. As a result, the entire line super capacitor be modelled using periodic boundary conditions [25].

Chapter 5

Comparison of Different Configuration

There are two kind designed supercapacitor cells arguments are used to simulate the thermal condition inside of the supercapacitor stack. One model has 5 mm angled distance between each cell outlet. Another model has 5 mm distance between cells and place horizontally. The air though into the module from the inlet which is the red arrows on the right to the outlet. Air flow in the individual cell gap flow after heat exchange, from the back of the vents out, the heat away, lower temperature rise, to achieve uniformity of temperature. However, the air comes along with the one axis. The individual supercapacitor cells which close to the exist have higher temperature than the inlet, because air has blocked by supercapacitor cell. In order to known the air flow rates, effect the thermal condition of the supercapacitor stack, three different air flow rates are applied (2,4 and 6 meter per second). There are three lines located on the model one to exam the temperature distribution for different location under different air flow rate. Based on those figures, it is clear to find out the temperature inside of the supercapacitor model for the model two is higher than the model one. The cells inside of the model two may have less performance, frequently maintain and less lifecycle.

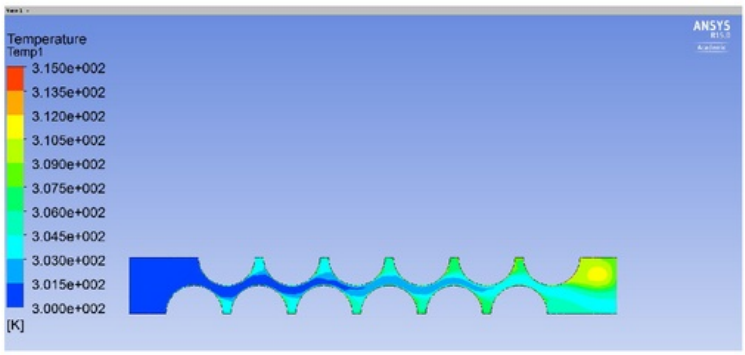

Figure 5.1: Model one temperature of the supercapacitor stack on 6 m per sec flow

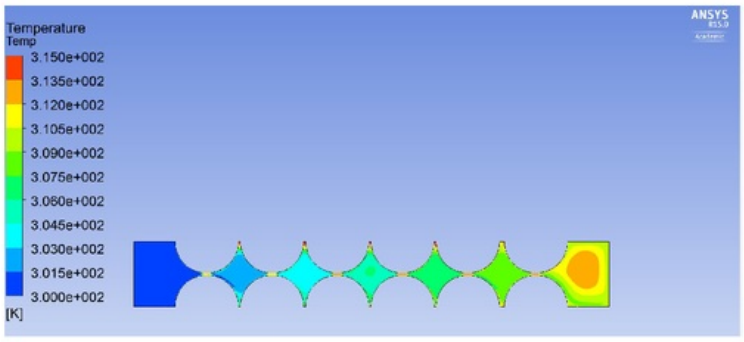

Figure 5.2: Model two temperature of the supercapacitor stack on 6 m per sec flow

Chapter 6

Conclusions and Future Work

6.1 Conclusions

This chapter is generally summaries the work has been done by doing final year thesis project heat transfer modelling of the supercapacitor stack and future lookout of the thermal modelling of the supercapacitor stack. The heat transfer models of the supercapacitor stacks have been made by simulation software. In order to achieve better performance of the supercapacitor stack, fans or cooling fluid may use to stabilise individual supercapacitor cells. That will increase the manufactory costs and reduce reliability of the supercapacitor stack. Even the best nature or force convention cooling solution could not found after this thesis project. The designed arrangements of supercapacitor cells made a significant improvement of the cooling method of supercapacitor stacks.

6.2 Future three dimensional model implementation

This thesis could be extended to a three dimensional model to simulate the different model supercapacitor stacks in commercial applications. Since the methodology to build and analysis two dimensional model has been established preciously, this implementation is easy to apply. However, more experiment time required and resources needed to simulation thermal condition of three dimensional supercapacitor model models. The CAD model for the three dimensional model has been made based on MAXXWELL supercapacitor stack which shown on Appendix [23].

Appendix A

Supercapacitor Stark

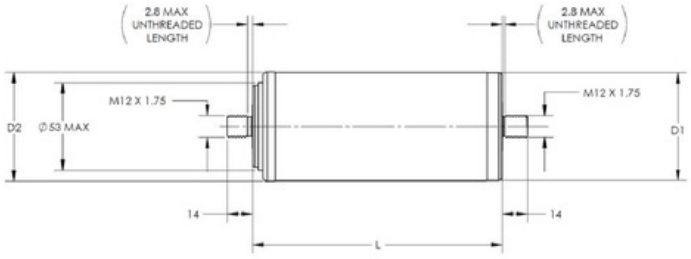

Part Description	Dimensions (mm) L (±0.3mm)	D1 (±0.2mm)	D2 (±0.7mm)	Package Quantity
BCAP3000 P300 K04	138	60.4	60.7	15

Figure A.1: supercapacitor cell.

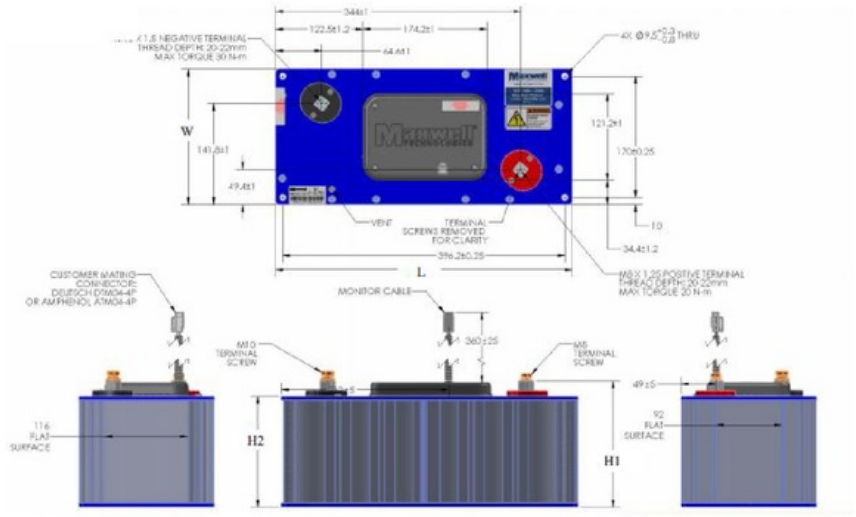

Part Description	Dimensions (mm) L (max)	W (max)	H1 (max)	H2 (max)	Package Quantity
BMOD0165 P048 C01	418	194	179	157	1

Figure A.2: supercapacitor stack dimetion.

PRODUCT SPECIFICATIONS

ELECTRICAL	BMOD0165 P048 C01
Rated Capacitance[1]	165 F
Minimum Capacitance, initial[1]	165 F
Maximum Capacitance, initial[1]	198 F
Maximum ESR $_{DC}$, initial[1]	6.0 mΩ
Test Current for Capacitance and ESR $_{DC}$[1]	100 A
Rated Voltage	48 V
Stored Energy[4]	53 Wh
Absolute Maximum Voltage[2]	51 V
Absolute Maximum Current	1,900 A
Maximum Series Voltage	750 V
Capacitance of Individual Cells[8]	3,000 F
Stored Energy, Individual Cell[8]	3.0 Wh
Number of Cells	18
TEMPERATURE	
Operating Temperature (Cell Case Temperature)	
Minimum	-40°C
Maximum	65°C
Storage Temperature (Stored Uncharged)	
Minimum	-40°C
Maximum	70°C

Figure A.3: Product Specifications for supercapacitor stack.

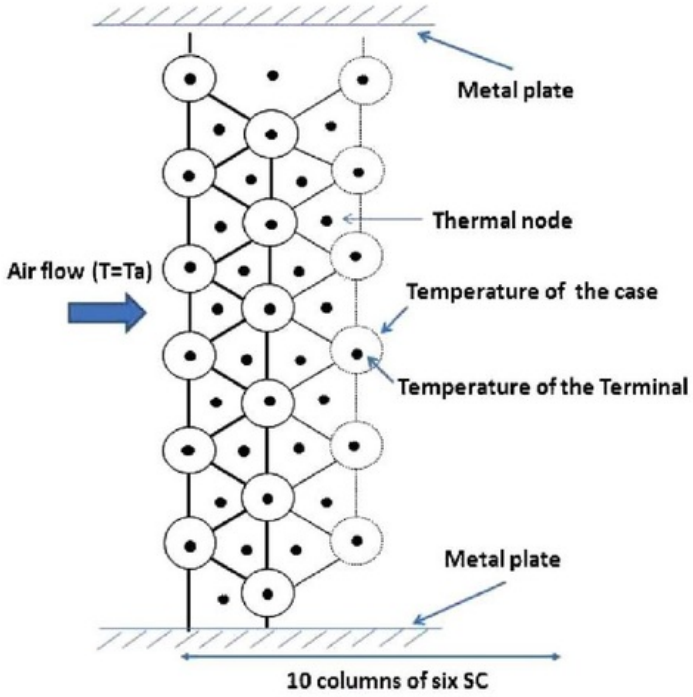

Figure A.4: 10 colume of 6 supercapacitor Stack.

Appendix B

Results

B.1 Mesh by ANSYS Workbench

The meshs generated by ANSYS Workbench are lisyed on this section.
The zoom in detail of the mesha is shown ,

B.2 Temperature of for different arrangments

Table B.1: Mesh configuration

Arrangement	Number of nodes	Number of elements
1	4719	6845
2	10484	27860

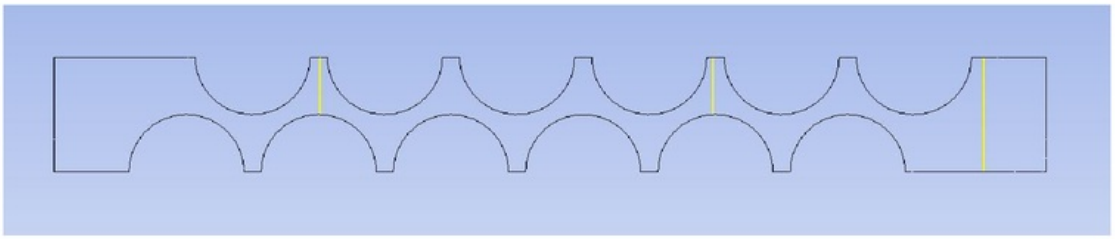

Figure B.1: Lines loacation.

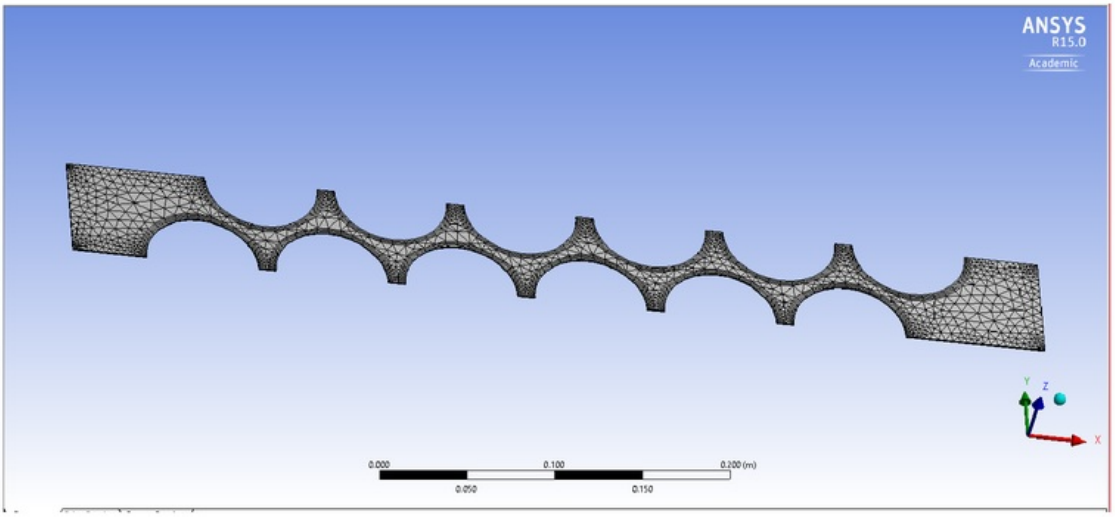

Figure B.2: Mesh generated by ANSYS Workbench

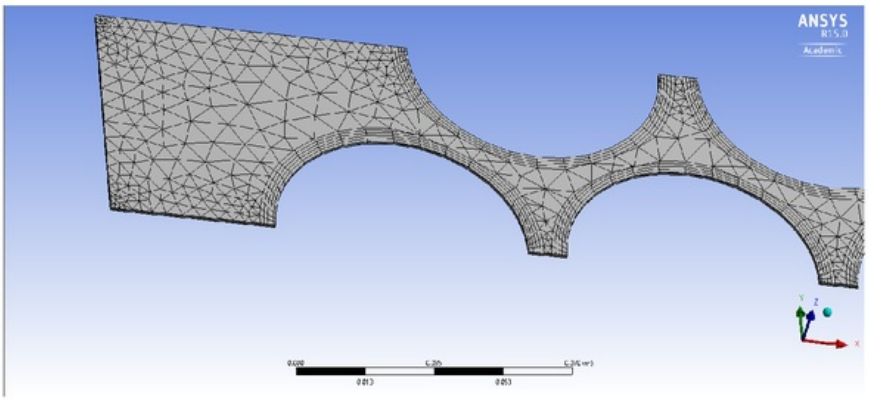

Figure B.3: Mesh generated by ANSYS Workbench

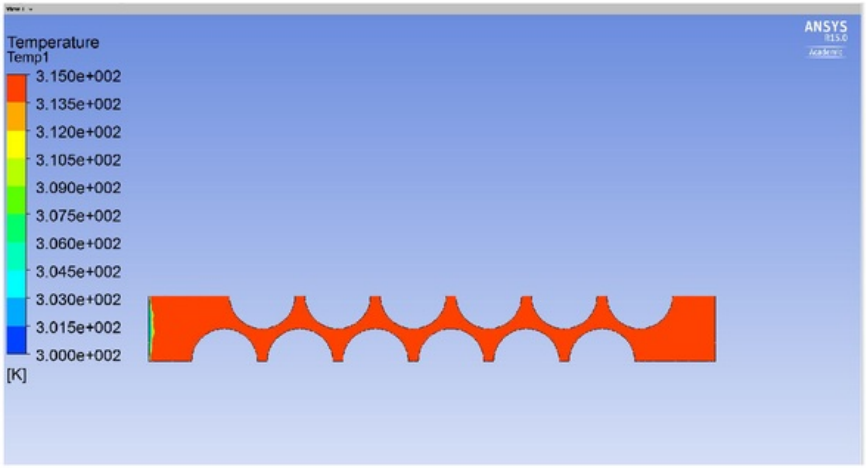

Figure B.4: Temperature of the model under $0m \setminus s^2$

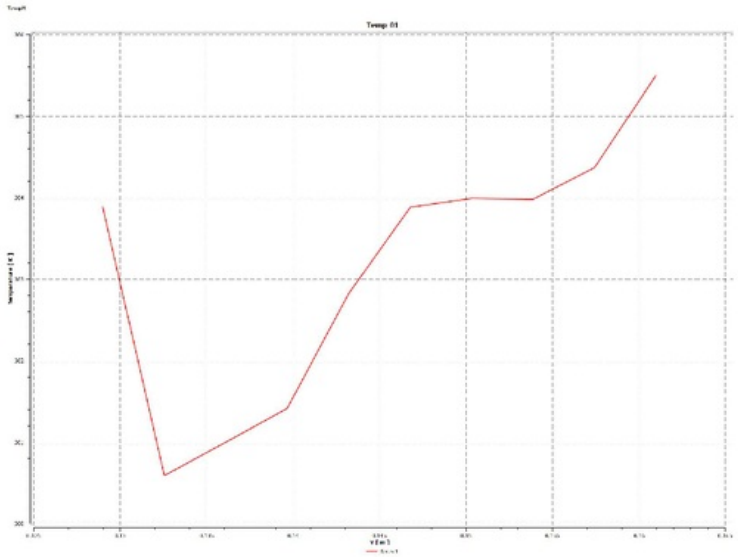

Figure B.5: Line 1, 2 meter per sec

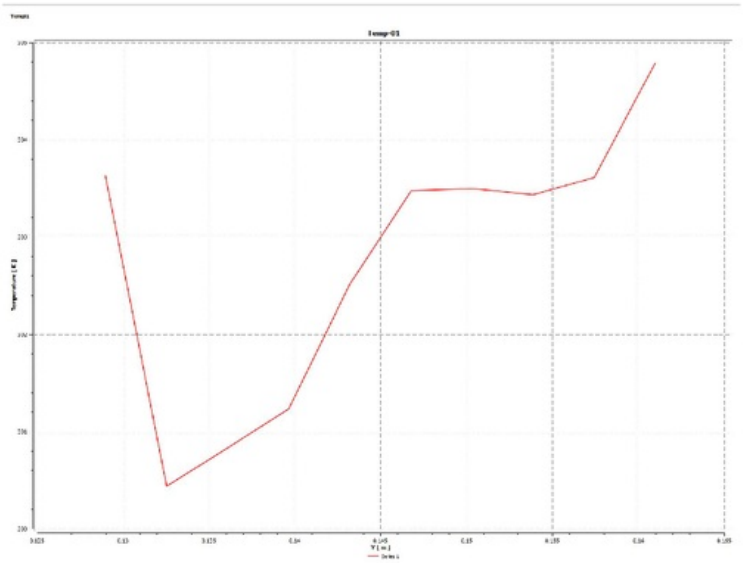

Figure B.6: Line 1, 4 meter per sec

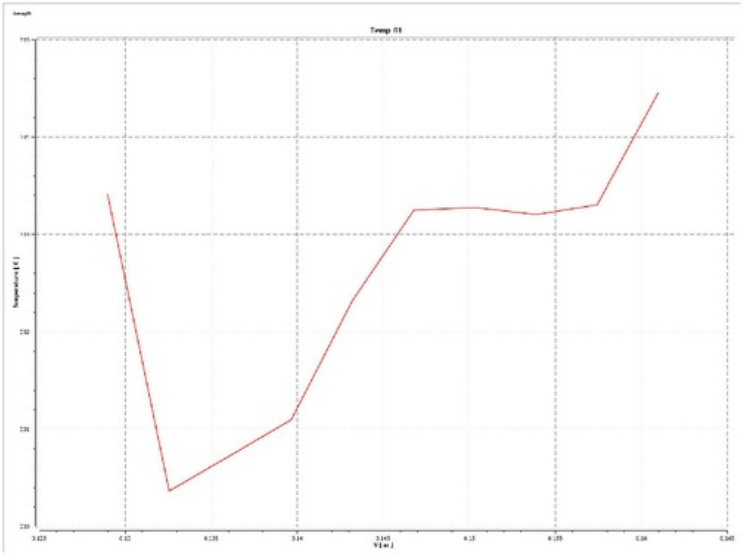

Figure B.7: Line 1, 6 meter per sec

Bibliography

[1] I. Voicu, H. Louahlia, H. Gualous, and R. Gallay. Thermal management and forced air-cooling of supercapacitors stack. *Applied Thermal Engineering*, 85:89–99, 2015. cited By 1.

[2] R. Haddad, A. El Shahat, and Y. Kalaani. Lead acid battery modeling for photovoltiac applications. *Journal of Electrical Engineering*, 15(2):17–24, 2015. cited By 2.

[3] J. Tu, G.H. Yeoh, and C. Liu. *Computational Fluid Dynamics: A Practical Approach*. Elsevier Science, 2007.

[4] F. Zhang, Y. Lu, X. Yang, L. Zhang, T. Zhang, K. Leng, Y. Wu, Y. Huang, Y. Ma, and Y. Chen. A flexible and high-voltage internal tandem supercapacitor based on graphene-based porous materials with ultrahigh energy density. *Small*, 10(11):2285–2292, 2014. cited By 20.

[5] J.A. Staser and J.W. Weidner. Mathematical modeling of hybrid asymmetric electrochemical capacitors. *Journal of the Electrochemical Society*, 161(8), 2014. cited By 8.

[6] K. Wang, L. Zhang, B. Ji, and J. Yuan. The thermal analysis on the stackable supercapacitor. *Energy*, 59:440–444, 2013. cited By 19.

[7] D. De, C. Klumpner, C. Patel, K. Ponggorn, M. Rashed, and G. Asher. Modelling and control of a multi-stage interleaved dc-dc converter with coupled inductors for super-capacitor energy storage system. *IET Power Electronics*, 6(7):1360–1375, 2013. cited By 17.

[8] M. Kim, Y. Hwang, and J. Kim. Graphene/mno2-based composites reduced via different chemical agents for supercapacitors. *Journal of Power Sources*, 239:225–233, 2013. cited By 73.

[9] J. Zhang and X.S. Zhao. On the configuration of supercapacitors for maximizing electrochemical performance. *ChemSusChem*, 5(5):818–841, 2012. cited By 150.

[10] X. Zhou, C. Peng, and G.Z. Chen. 20 v stack of aqueous supercapacitors with carbon (-), titanium bipolar plates and cnt-polypyrrole composite (+). *AIChE Journal*, 58(3):974–983, 2012. cited By 14.

[11] C.-C. Liu, D.-S. Tsai, W.-H. Chung, K.-W. Li, K.-Y. Lee, and Y.-S. Huang. Electrochemical micro-capacitors of patterned electrodes loaded with manganese oxide and carbon nanotubes. *Journal of Power Sources*, 196(13):5761–5768, 2011. cited By 43.

[12] P. Kulsangcharoen, C. Klumpner, M. Rashed, and G. Asher. A new duty cycle based efficiency estimation method for a supercapacitor stack under constant power operation. volume 2010, 2010. cited By 0.

[13] Y. Lu. Electroless copper plating on 3-mercaptopropyltriethoxysilane modified pet fabric challenged by ultrasonic washing. *Applied Surface Science*, 255(20):8430–8434, 2009. cited By 25.

[14] J. Jin, Z. Dong, J. He, R. Li, and J. Ma. Synthesis of novel porphyrin and its complexes covalently linked to multi-walled carbon nanotubes and study of their spectroscopy. *Nanoscale Research Letters*, 4(6):578–583, 2009. cited By 9.

[15] Yu X. Tu J. Becker, W. A generalised cfd learning and prediction system. volume 2, pages 615–620, 2007. cited By 0.

[16] Yu X. Tu J. Becker, W. An adaptive grid method and its application to cfd learning and prediction. pages 1467–1472, 2008. cited By 0.

[17] Tu J. Subic A. Li H. Ilie K. Abu-Hijleh, B. Cfd comparison of clearance flow in a rotor-casing assembly using asymmetric vs. symmetric lobe rotors. volume 259, pages 327–330, 2003.

[18] Inthavong K. Yang W. Tu J. Fung, M.C. Cfd modeling of spray atomization for a nasal spray device. *Aerosol Science and Technology*, 46(11):1219–1226, 2012. cited By 5.

[19] Tian Z.F. Tu J.Y. Inthavong, K. Cfd simulations on the heating capability in a human nasal cavity. pages 842–847, 2007. cited By 4.

[20] Tu J.Y. Yeoh G.H. Tian, Z.F. Cfd studies of indoor airflow and contaminant particle transportation. *Particulate Science and Technology*, 25(6):555–570, 2007. cited By 13.

[21] Inthavong K. Mohanarangam K. Petersen P. Yang W. Tu J. Tao, Y. Cfd study of human-induced wake and particle dispersion in indoor environment. volume 2, pages 733–740, 2015. cited By 0.

[22] Fletcher C.A.J. Tu J.Y. Nguyen, A.V. Cfd study of the heat transfer between a dilute gas particle suspension flow and an obstruction. *Numerical Heat Transfer; Part A: Applications*, 35(5):537–551, 1999. cited By 4.

[23] Li X. Yang L. Tu J. Yan, Y. Evaluation of manikin simplification methods for cfd simulations in occupied indoor environments. *Energy and Buildings*, 127:611–626, 2016. cited By 0.

[24] Ren C. Sun Y. Tu J. Yang X. Wang, S. Experimental and numerical investigation of the flow measurement method utilized in the steam generator of htr-pm. *Nuclear Engineering and Design*, 305:191–199, 2016. cited By 0.

[25] Fletcher C.A.J. Lee B.E. Tu J.Y. Kouzoubov, A. Gas-solid confined flows with heat transfer. volume 17, 1997. cited By 0.

[26] Tu J. Cheung C.P. Beare R. Phan T. Reutens D. Thien F. Ding, S. Geometric model generation for cfd simulation of blood and air flows. pages 1335–1338, 2007. cited By 3.

[27] M. Kim and J. Kim. Development of high power and energy density microsphere silicon carbide-mno2 nanoneedles and thermally oxidized activated carbon asymmetric electrochemical supercapacitors. *Physical Chemistry Chemical Physics*, 16(23):11323–11336, 2014. cited By 31.

[28] Inthavong K. Tu J.Y. Ge, Q.J. Local deposition fractions of ultrafine particles in a human nasal-sinus cavity cfd model. *Inhalation Toxicology*, 24(8):492–505, 2012. cited By 8.

[29] Wong K.K.L. Tu J. Dong, J. Hemodynamics analysis of patient-specific carotid bifurcation: A cfd model of downstream peripheral vascular impedance. *International Journal for Numerical Methods in Biomedical Engineering*, 29(4):476–491, 2013. cited By 15.

[30] Tu J. Heschl C. Inthavong, K. Micron particle deposition in the nasal cavity using the v 2-f model. pages 383–388, 2011. cited By 0.

[31] Cheung S.C.P. Yeoh G.H. Tu J. Deju, L. Study of isothermal vertical bubbly flow using direct quadrature method of moments. *Journal of Computational Multiphase Flows*, 4(1):23–40, 2012. cited By 3.